Hindawi
International Journal of Antennas and Propagation
Volume 2018, Article ID 8075318, 8 pages
https://doi.org/10.1155/2018/8075318

*Research Article*

# Synthesis of the Sparse Uniform-Amplitude Concentric Ring Transmitting Array for Optimal Microwave Power Transmission

**Hua-Wei Zhou, Xue-Xia Yang, and Sajjad Rahim**

*Shanghai Institute of Advanced Communication and Data Science, Key laboratory of Specialty Fiber Optics and Optical Access Networks, Joint International Research Laboratory of Specialty Fiber Optics and Advanced Communication, Shanghai University, Shanghai 200444, China*

Correspondence should be addressed to Xue-Xia Yang; yang.xx@shu.edu.cn

Received 8 March 2018; Revised 16 May 2018; Accepted 6 June 2018; Published 8 July 2018

Academic Editor: Ikmo Park



Beam capture efficiency (*BCE*) is one key factor of the overall efficiency for a microwave power transmission (MPT) system, while sparsification of a large-scale transmitting array has a practical significance. If all elements of the transmitting array are excited uniformly, the fabrication, maintenance, and feed network design would be greatly simplified. This paper describes the synthesis method of the sparse uniform-amplitude transmitting array with concentric ring layout using particle swarm optimization (PSO) algorithm while keeping a higher *BCE*. Based on this method, uniform exciting strategy, reduced number of elements, and a higher *BCE* are achieved simultaneously for optimal MPT. The numerical results of the sparse uniform-amplitude concentric ring arrays (SUACRAs) optimized by the proposed method are compared with those of the random-located uniform-amplitude array (RLUAA) and the stepped-amplitude array (SAA), both being reported in the literatures for the maximum *BCE*. Compared to the RLUAA, the SUACRA saves 32% elements with a 1.1% higher *BCE*. While compared to the SAA, the SUACRA saves 29.1% elements with a bit higher *BCE*. The proposed SUACRAs have higher *BCE*s, simple array arrangement and feed network, and could be used as the transmitting array for a large-scale MPT system.

## 1. Introduction

Microwave power transmission (MPT) technology transfers power from one location to another by the microwave beam, which could be applied in supplying power to the space power satellites, unmanned aerial vehicles, the far-reached areas, and so on [1]. For a large-scale MPT system, the most important parameter is the beam capture efficiency (*BCE*), which is the ratio of the captured microwave power by the receiving antenna array to the transmitted power by the transmitting antenna array [2].

In 1974, Dr. Brown performed an MPT experiment with a distance of 1.7 m in the laboratory. The overall efficiency up to 54% and the *BCE* is 95% [3]. However, the MPT experiment carried out next year only obtained an overall efficiency of 7% and *BCE* of 11.3% when the range was 1.54 km [4]. Until now, the overall efficiency of a MPT system is not higher than 10% because of a low *BCE* [2].

The transmitting aperture illuminated by the Gaussian amplitude distribution can obtain a maximum beam capture efficiency $BCE^{\max}$ higher than 99% because of the broad beam width and low side lobe level in the far field [5]. Discrete transmitting aperture, namely, antenna array, is more practical for expanding the MPT system to a large scale. The optimized excitation amplitudes of a planar array for the $BCE^{\max}$ can be achieved by solving generalized eigenvalue problem [6]. Nevertheless, owing to the continuous amplitude distribution, many different amplifiers would be required for every distinct element, which results in a complex transmitting array. To reduce the kinds of amplifiers, Baki et al. and Li et al. [7, 8] proposed the isosceles trapezoidal distribution (ITD) and stepped-amplitude arrays (SAAs), respectively. The design and implementation of transmitting array could be greatly simplified if all elements are uniformly excited [9]. The random-located uniform-amplitude array (RLUAA) comprising of 100 elements was

optimized by particle swarm optimization (PSO) algorithm with a *BCE* of 89.96% being obtained [10]. However, the computation amount would grow up rapidly as the element number increases, which could not be applied in a large-scale transmitting array design.

Besides the exciting strategy, the sparsification of a large-scale transmitting array has a practical significance. Sparse arrays can not only reduce the complexity of the feed networks but also can decrease the weight. Most studies on sparse antenna arrays [11–13] are focused on reducing the number of elements, the peak side lobe level, the computational effort, and so on but not considering the power transmission efficiency. In the MPT scenario, the element numbers of antenna arrays were reduced to 65% and 64% of the original one through compressive sensing (CS) and convex programming (CP) methods, respectively, in [14, 15]. By combining these two methods, the element number was reduced to 54% of the original one and the *BCE* was improved about 3.16% [16]. Unfortunately, arrays in [14–16] were not uniformly illuminated. Moreover, CS and CP would not be efficient for the large-scale array design due to strong nonlinear relationship between the array factor and the element positions [17]. The Bessel-approximation array factor of a concentric ring array (CRA) is only related to the radius and excitation of each ring, which would reduce the computation amount and could be used in optimizing a large-scale array.

PSO algorithm was firstly introduced by Kennedy and Eberhart in 1995 [18]. Due to its high search efficiency, PSO has been widely used in enhancing antenna gain [19] and beam pattern synthesis [20] and improving *BCE* of a MPT system [10]. In this work, the synthesis of the sparse uniform-amplitude transmitting array is discussed for the optimal MPT. The exciting strategy, element number, and *BCE* are considered simultaneously for the MPT system. The outline of this paper is organized as follows. Section 2 describes the calculation equations of *BCE* of the sparse uniform-amplitude CRA (SUACRA). Section 3 introduces the optimization model for the SUACRA, and Section 4 presents the numerical results of SUACRAs, which have been compared with those of RLUAA discussed in [10] and SAA proposed in [8].

## 2. Theoretical Foundation

As shown in Figure 1, the transmitting array is a CRA located in the XOY plane with an element in the center, and the radial space between the $(m-1)$th and the $m$th rings is denoted by $\Delta\rho_m$ $(m = 1, \ldots, M)$. All elements are excited by the identical phase and amplitude.

The receiving array is in the far region of the transmitting array, namely, $D_{tr} \geq 2D_t^2/\lambda$, where $D_{tr}$ is the distance between transmitting and receiving array, $D_t$ is the radius of transmitting array, and $\lambda$ is the wavelength. As a result, the CRA array factor can be written as [21]

$$AF = \sum_{m=0}^{M} F_m = \sum_{m=0}^{M} \sum_{n=1}^{N_m} I_m \exp\left[ju_m \cos\left(\varphi - \varphi_{mn}\right)\right], \quad (1)$$

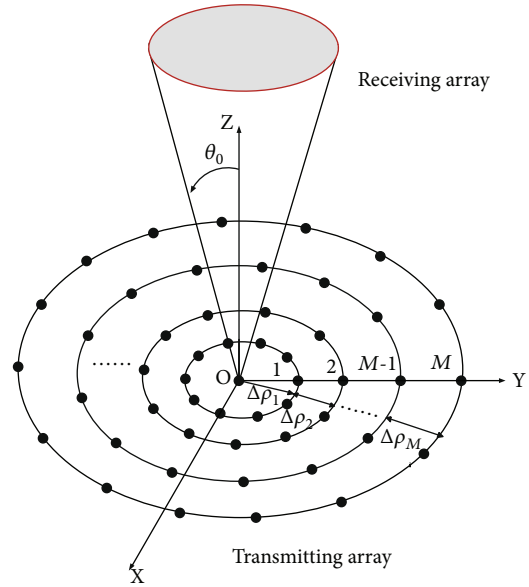


Figure 1: Geometry of the MPT system.

$$u_m = k\rho_m \sin\theta, \quad (2)$$

$$\rho_m = \sum_{i=1}^{m} \Delta\rho_i, \quad (3)$$

where $F_m$ is the array factor of $m$th ring, $\rho_m$, $N_m$, and $I_m$ represent the radius, the element number and the excitation amplitude of the $m$th ring, respectively, $k$ denotes the wavenumber, and $\varphi_{mn}$ is the azimuth angle of the $n$th element located on the $m$th ring.

$N_m$ elements are distributed with the same space on the $m$th ring. When $N_m$ is large enough, array factor of the $m$th ring can be approximated as [21]

$$F_m \approx T_m J_0(u_m). \quad (4)$$

In (4), $T_m = I_m N_m$ and $J_0$ is the zero-order Bessel function of the first kind. To evaluate the precision, the power error index $\varsigma_m$ is defined as

$$\xi_m = 10 \log\left\{\frac{\int_\Omega \left[|F_m|^2 - |T_m J_0(u_m)|^2\right] d\Omega}{\int_\Omega |F_m|^2 d\Omega}\right\}, \quad (5)$$

where $\Omega$ is the visible region $(0 \leq \theta \leq \pi,\ 0 \leq \varphi \leq 2\pi)$ of the transmitting array. Under the constraint of keeping a higher precision of (4), the minimum element number $N_m^{\min}$ can be found by increasing $N_m$ from 2 till to reach $\varsigma_m \leq -30$ dB. The line labeled by numerical results in Figure 2 lays out the $N_m^{\min}$ for radiuses ranging from $0.5\lambda$ to $19.5\lambda$ with an interval of $0.5\lambda$.

By applying the fitting method, $N_m^{\min}$ can be approximated to the following formula:

$$N_m^{\min} = \lceil 3 + 6.7\rho_m \rceil, m \neq 0, \quad (6)$$

where "$\lceil\ \rceil$" stands for mapping number to the least integer that is greater than or equal to the original number. The

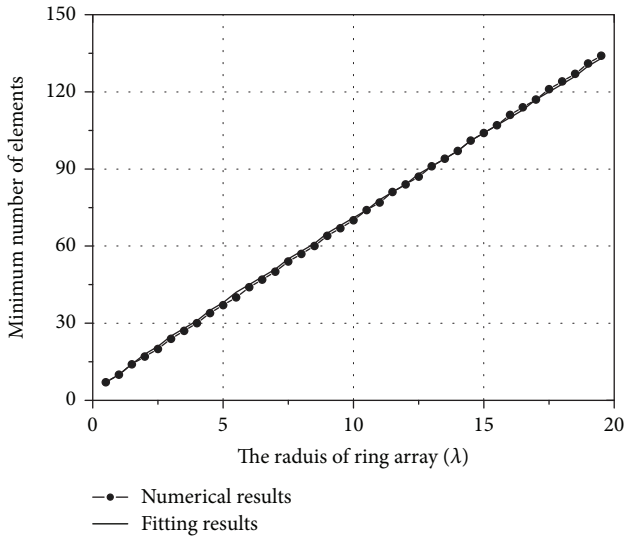


Figure 2: The minimum element number on different radiuses for the constraint of $\varsigma_m \le -30$ dB.

fitting line is plotted in Figure 2. It can be seen that the fitting results are consistent well with the numerical results. Equation (6) could be used to estimate $N_m^{\min}$ on a ring of a large-scale array.

With the element numbers on each ring not less than the minimum ones, namely, $N_m \ge N_m^{\min}$ $(m = 1, \dots, M)$, the CRA array factor of (1) can be rewritten as

$$AF = \mathbf{T}\mathbf{J}^H, \tag{7}$$

where $\boldsymbol{T} = [T0, T1, \dots, TM]$, $\mathbf{J} = [J_0(u_0), J_0(u_1), \dots, J_0(u_M)]$, and superscript "$H$" stands for transpose and complex conjugate. The CRA power pattern is

$$S = |F|^2 = \mathbf{T}\mathbf{J}^H\mathbf{J}\mathbf{T}^H. \tag{8}$$

Therefore, the *BCE* can be calculated by the following formula:

$$BCE = \frac{P_\Psi}{P_\Omega} = \frac{\int_\Psi S d\Psi}{\int_\Omega S d\Omega} = \frac{\mathbf{T}\mathbf{A}\mathbf{T}^H}{\mathbf{T}\mathbf{B}\mathbf{T}^H}, \tag{9}$$

where $\Psi$ shows the receiving region, $P_\Psi$ is the received power, and $P_\Omega$ is the total transmitting power. $\mathbf{A}$ and $\mathbf{B}$ are all $(M+1)\times(M+1)$ matrixes. The elements of $\mathbf{A}$ and $\mathbf{B}$ are calculated as

$$\begin{aligned} \mathbf{A}_{pq} &= \int_\Psi J_0(u_p) J_0(u_q) d\Psi, \\ \mathbf{B}_{pq} &= \int_\Omega J_0(u_p) J_0(u_q) d\Omega. \end{aligned} \tag{10}$$

In the above equations, $p = 0, 1, \dots, M$ and $q = 0, 1, \dots, M$. Considering the uniform exciting strategy, namely, $I_m = 1$ for $m = 0, 1, \dots, M$, $\mathbf{T}$ can be simplified as $\mathbf{T} = \mathbf{N} = [1, N_1, \dots, N_M]$. $\mathbf{N}$ is the element number matrix. The *BCE* of the uniform-amplitude transmitting array, denoted by $BCE^{\mathrm{U}}$, can be achieved by

$$BCE^{\mathrm{U}} = \frac{\mathbf{N}\mathbf{A}\mathbf{N}^H}{\mathbf{N}\mathbf{B}\mathbf{N}^H}. \tag{11}$$

When the $\Psi$ is defined, the matrices of $\mathbf{A}$ and $\mathbf{B}$ can be calculated from $\mathbf{u} = [u_0, u_1, \dots, u_M]$. According to (2), $\mathbf{u}$ is directly determined by applying the radial space matrix $\boldsymbol{\Delta\rho} = [\Delta\rho_1, \Delta\rho_2, \dots, \Delta\rho_M]$. Therefore, from the given $\boldsymbol{\Delta\rho}$ and $\mathbf{N}$, the $BCE^{\mathrm{U}}$ can be calculated by using (11).

Table 1: Performance comparison of the SUACRA 1, 2, and the RLUAA.

| | RLUAA [10] | This work | |
|---|---|---|---|
| | | SUACRA 1 | SUACRA 2 |
| *BCE* | 89.96% | 91.06% | 90.08% |
| Element number | 100 | 68 | 56 |
| Sparsification ratio | 0 | 32% | 44% |

## 3. Optimization Model of SUACRA

Sparsification ratio $\xi$ of a transmitting array is defined as the ratio of the saved element number of the sparse array to that of the original one. In this paper, the radial space matrix $\boldsymbol{\Delta\rho}$ and the element number matrix $\mathbf{N}$ are simultaneously optimized to improve the $\xi$ at the most extent while the $BCE^{\mathrm{U}}$ is kept as high as possible. The optimization model can be established as follows:

$$\mathrm{Find}[\Delta\rho_1, \dots, \Delta\rho_M, N_1, \dots, N_M], \tag{12}$$

$$\text{Max. fitness} = \left(w_B BCE^{\mathrm{U}} + w_\xi \xi\right) + p_B h_B, \tag{13}$$

$$\text{S.T. } \Delta\rho_m \ge d^{\min}, \quad m = 1, 2, \dots, M, \tag{14}$$

where $w_B$ and $w_\xi$ are weights of the $BCE^{\mathrm{U}}$ and $\xi$, respectively, and $w_B + w_\xi = 1$. In order to investigate the impact of $BCE^{\mathrm{U}}$ on the $\xi$, the penalty factor $p_B$ and penalty function $h_B$ have been introduced in (13). The $h_B$ is defined as

$$h_B = \min\left(BCE^{\mathrm{U}} - BCE_0, 0\right). \tag{15}$$

$BCE_0$ in (15) is the threshold value of $BCE^{\mathrm{U}}$, which is set to be 1% lower than the maximum $BCE^{\mathrm{U}}$ of the SUACRA, as denoted by $BCE^{\mathrm{Umax}}$.

From (15), $h_B < 0$ when $BCE^{\mathrm{U}} < BCE_0$. In order to maintain $BCE^{\mathrm{U}} \ge BCE_0$, $p_B$ should be large enough, such as $10^5$, to magnify the impact of the $h_B$ on the *fitness* function. In this way, $h_B$ could change toward zero in the PSO procedure. Otherwise, $p_B$ should be set to zero to invalidate the $h_B$.

The radial space $\Delta\rho_m$ should not be less than $d^{\min}$ and can be guaranteed by (14), where $d^{\min}$ is the minimum space between the adjacent elements on the planar array. In order to ensure the space along ring path between the adjacent

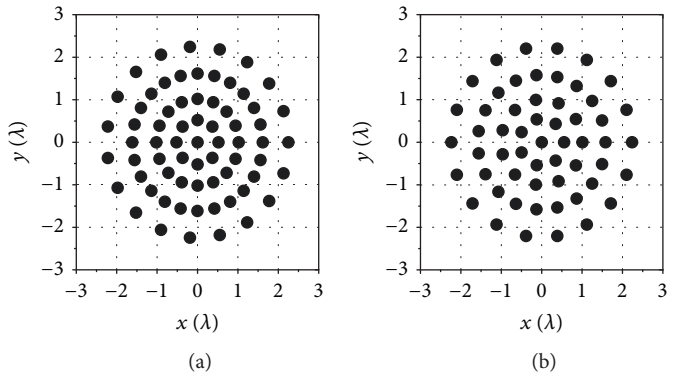


Figure 3: Layouts of the SUACRA 1 and 2: (a) SUACRA 1 (68 elements) and (b) SUACRA 2 (56 elements).

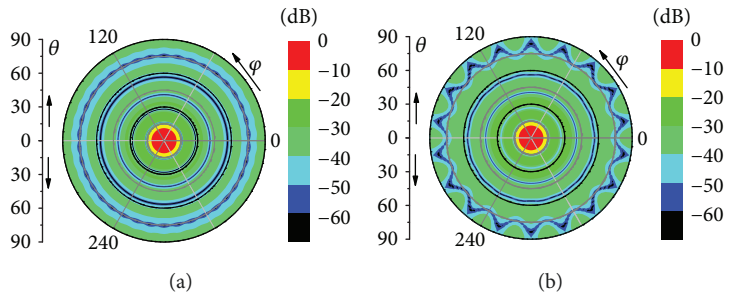


Figure 4: Power patterns of SUACRA 1 and 2: (a) SUACRA 1 and (b) SUACRA 2.

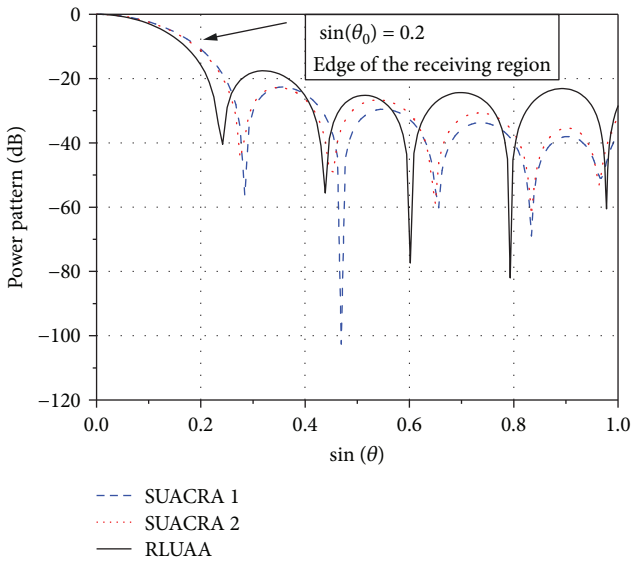


Figure 5: Power patterns ($\varphi = 0$) comparison of SUACRA 1, 2, and the RLUAA.

elements larger than $d^{\min}$, the element number of $m$th ring $N_m$ should satisfy this condition:

$$N_m \le N_m^{\max} = \left\lfloor \frac{2\pi\rho_m}{d^{\min}} \right\rfloor, \quad m \ne 0, \tag{16}$$

where "$\lfloor\ \rfloor$" stands for mapping number to the greatest integer that is less than or equal to the original number. $N_m$ should not be less than $N$ min $m$ to keep the accuracy of (4), namely, power error index $\varsigma_m \le -30$ dB. Moreover, the size of SUACRA is confined by $\rho_M \le D_t/2$, in which $D_t$ is the expected maximum diameter.

Table 2: Initial and optimized parameters of SUACRA 1 and 2.

| $M$ | Initial | | SUACRA 1 | | SUACRA 2 | |
|---|---|---|---|---|---|---|
| | $\Delta\rho_m$ ($\lambda$) | $N_m$ | $\Delta\rho_m$ ($\lambda$) | $N_m$ | $\Delta\rho_m$ ($\lambda$) | $N_m$ |
| 1 | 0.4 | 6 | 0.52 | 8 | 0.55 | 7 |
| 2 | 0.4 | 9 | 0.50 | 16 | 0.45 | 11 |
| 3 | 0.4 | 12 | 0.60 | 24 | 0.58 | 19 |
| 4 | 0.4 | 14 | 0.64 | 19 | 0.65 | 18 |
| 5 | 0.4 | 17 | 0.40 (del) | 30 (del) | 0.41 (del) | 31 (del) |

The variable set is $[\Delta\rho_1, \ldots, \Delta\rho_M, N_1, \ldots, N_M]$, while the fitness function is stated in (13). Each particle of the swarm characterizes a candidate solution, which can be evaluated by the fitness function. After each iteration, the optimal particle is obtained, and each particle is updated. When the termination condition is satisfied, the optimal variable values can be obtained as the optimal particle over the iteration history. For details of the PSO, readers could refer to [20] and the references therein.

## 4. Numerical Results

The SUACRAs are optimized by the proposed procedure and method. The numerical results will be compared with those of the RLUAA in [10] and the SAA in [8] on the condition

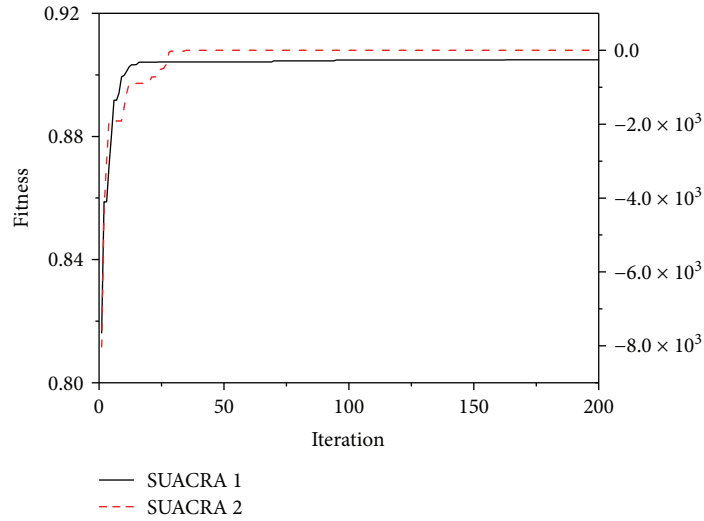


Figure 6: The fitness values throughout the optimization process of SUACRA 1 and 2.

of the same transmitting aperture size and the same inception angle.

*4.1. Synthesis of the SUACRA Compared with the RLUAA.* The RLUAA, the first model optimized in [10], consists of 100 elements distributed arbitrarily on an aperture of $4.5\lambda \times 4.5\lambda$, in which the minimum element distance $d^{\min}$ was $0.4\lambda$ and the inception angle was $\theta_0 = 0.201$. The optimization of the SUACRA is carried out for the same transmitting aperture and the same inception angle, which is denoted by SUACRA 1. In order to further improve the sparsification ratio of $\xi$, the SUACRA 2 is investigated with a 1% decrease of $BCE^{\mathrm{U}}$ compared to that of SUACRA 1. The numerical results are listed in Table 1, and the layouts of SUACRA 1 and 2 are given in Figure 3.

In order to improve the sparsification ratio of $\xi$ and keep $BCE^{\mathrm{U}}$ as high as possible, in the optimization of SUACRA 1, $w_B$ and $w_\xi$ are set to 0.99 and 0.01, respectively. Penalty factor $p_B$ is set as 0 to invalidate $h_B$. As shown in Table 1, SUACRA 1 has a $BCE^{\mathrm{U}}$ of 91.06%. Compared to the RLUAA, SUACRA 1 saves 32% elements and has a 1.1% higher $BCE^{\mathrm{U}}$.

With 1% decrease of $BCE^{\mathrm{U}}$ of SUACRA 1, the threshold of $BCE_0$ is set to 90.06%. In order to improve $\xi$ at the most extent, $w_B$ and $w_\xi$ are set to 0 and 1, respectively. The penalty factor $p_B$ is set as $10^5$ to guarantee $BCE^{\mathrm{U}} \geq BCE_0$. The numerical results show that the $\xi$ of the SUACRA 2 is improved by 12% with 0.98% decrease of $BCE^{\mathrm{U}}$, which means that the element number is reduced to 56% of the original RLUAA.

As shown by the SUACRAs' power patterns given in Figure 4, SUACRAs can concentrate microwave power on the receiving region. When $\theta$ is close to $\pi/2$, the pattern of SUACRA 2 is not symmetrical with respect to the center ($\theta = 0$, $\varphi = 0$), because the element numbers of rings is close to the minimum ones. Nevertheless, the difference is just 0.15% between the accurate *BCE* (90.08% obtained by (1)) and the approximate one (90.23% obtained by (7)). Moreover, the power patterns ($\varphi = 0$) comparison of two SUACRAs and the original RLUAA are given in Figure 5.

Table 3: Performance comparison of the SUACRA 3, 4, and the SAA.

| | SAA [8] | This work | |
|---|---|---|---|
| | | SUACRA 3 | SUACRA 4 |
| *BCE* | 92.51% | 92.53% | 91.53% |
| Element number | 316 | 224 | 193 |
| Sparsification ratio | 0 | 29.1% | 38.9% |

Compared to the RLUAA, the two SUACRAs have lower side lobes and higher main lobe levels. Therefore, the two SUACRAs have higher $BCE^{\mathrm{U}}$ of 91.06% and 90.08%, respectively. The side lobe of SUACRA 1 is a little bit lower than that of the SUACRA 2, which results in the difference of 0.98% $BCE^{\mathrm{U}}$.

The initial and optimized parameters of SUACRA 1 and 2 are given in Table 2. The initial $\Delta\rho_m$ and $N_m$ are set to $d^{\min}$ and $N_m^{\min}$, respectively. Because the diameter of the 6th ring of the initialized array will be larger than the maximum aperture size $4.5\lambda$, parameter $M$ is set as 5. The symbol "del" in Table 2 means that the according ring is deleted because the diameter of the ring is larger than $4.5\lambda$. In the optimization, the population size is set as 60. As shown in Figure 6, the fitness values of the two SUACRAs rapidly reach the convergence points within 50 iterations.

*4.2. Synthesis of the SUACRA Compared with the SAA.* The first discrete aperture example, namely, the SAA, in [8] consists of 316 elements distributed on a circular aperture of diameter $D_t = 9.5\lambda$, in which the inception angle $\theta_0$ was 0.107. The optimization of the SUACRA is carried out for the same transmitting aperture and the same inception angle, which is denoted by SUACRA 3. In order to further improve the sparsification ratio of $\xi$, the SUACRA 4 is investigated with 1% decrease of $BCE^{\mathrm{U}}$ compared to that of SUACRA 3. The numerical results are listed in Table 3, and the layouts of SUACRA 3 and 4 are given in Figure 7.

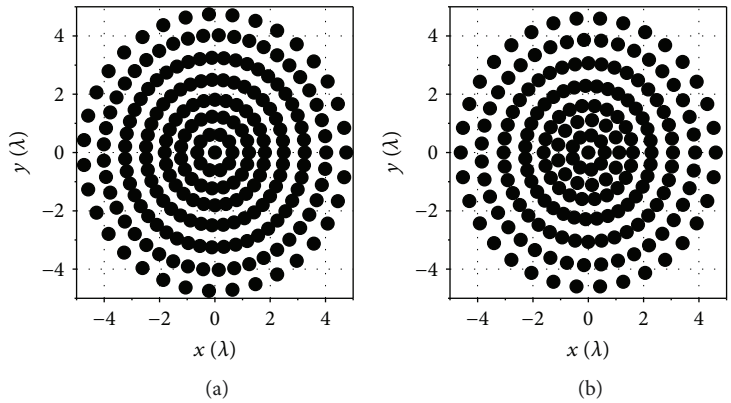


Figure 7: Layouts of the SUACRA 3 and 4: (a) SUACRA 3 (224 elements) and (b) SUACRA 4 (193 elements).

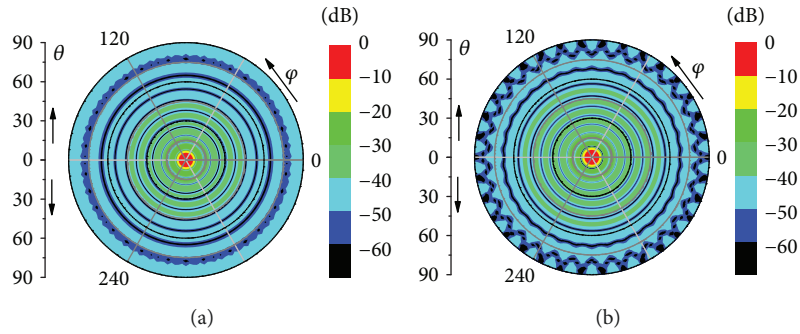


Figure 8: Power patterns of SUACRA 3 and 4: (a) SUACRA 3 and (b) SUACRA 4.

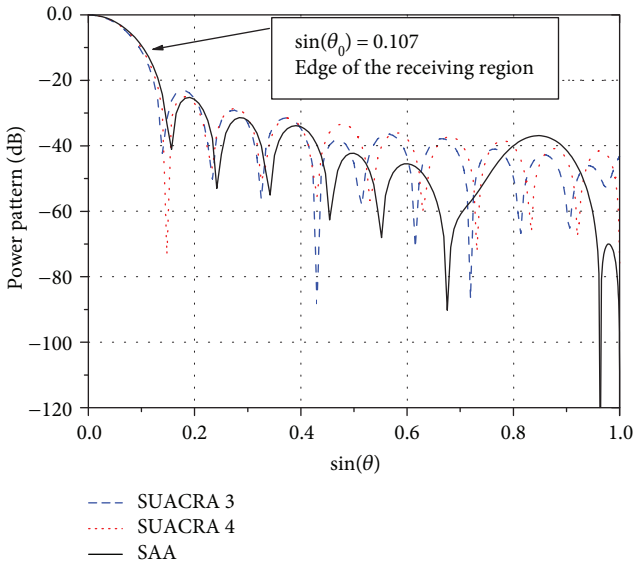


Figure 9: Power patterns ($\varphi = 0$) comparison of SUACRA 3, 4 and the SAA.

Compared to the SAA, SUACRA 3 saves 29.1% elements and has a bit higher $BCE^{U}$, while the $\xi$ of the SUACRA 4 is improved by 9.8% with 1% decrease of $BCE^{U}$.

The power patterns of SUACRA 3 and 4 are given in Figure 8, and the special power patterns ($\varphi = 0$) comparison of SUACRA 3, 4 and the original SAA are given in Figure 9. It could be seen that the main beams of the three arrays are almost the same although their side lobes are different. SUACRA 3 and the SAA have the same $BCE^{U}$ of 92.5%. The side lobe of SUACRA 4 is a little bit higher than that of SUACRA 3, which results in 1% decrease of $BCE^{U}$.

Table 4: Initial and optimized parameters of SUACRA 3 and 4.

| $M$ | Initial | | SUACRA 3 | | SUACRA 4 | |
|---|---|---|---|---|---|---|
| | $\Delta\rho_m$ ($\lambda$) | $N_m$ | $\Delta\rho_m$ ($\lambda$) | $N_m$ | $\Delta\rho_m$ ($\lambda$) | $N_m$ |
| 1 | 0.4 | 6 | 0.64 | 10 | 0.59 | 9 |
| 2 | 0.4 | 9 | 0.60 | 19 | 0.53 | 13 |
| 3 | 0.4 | 12 | 0.58 | 28 | 0.49 | 22 |
| 4 | 0.4 | 14 | 0.68 | 39 | 0.68 | 35 |
| 5 | 0.4 | 17 | 0.76 | 47 | 0.77 | 40 |
| 6 | 0.4 | 20 | 0.77 | 45 | 0.80 | 39 |
| 7 | 0.4 | 22 | 0.72 | 35 | 0.75 | 34 |
| 8 | 0.4 | 25 | 0.77 (del) | 40 (del) | 0.71 (del) | 39 (del) |
| 9 | 0.4 | 28 | 0.71 (del) | 45 (del) | 0.99 (del) | 46 (del) |
| 10 | 0.4 | 30 | 0.47 (del) | 48 (del) | 0.84 (del) | 52 (del) |
| 11 | 0.4 | 33 | 0.79 (del) | 54 (del) | 0.76 (del) | 57 (del) |

The initial and optimized parameters of SUACRA 3 and SUACRA 4 are given in Table 4. The parameter $M$ is set as 11, and the population size is set as 120. As shown in

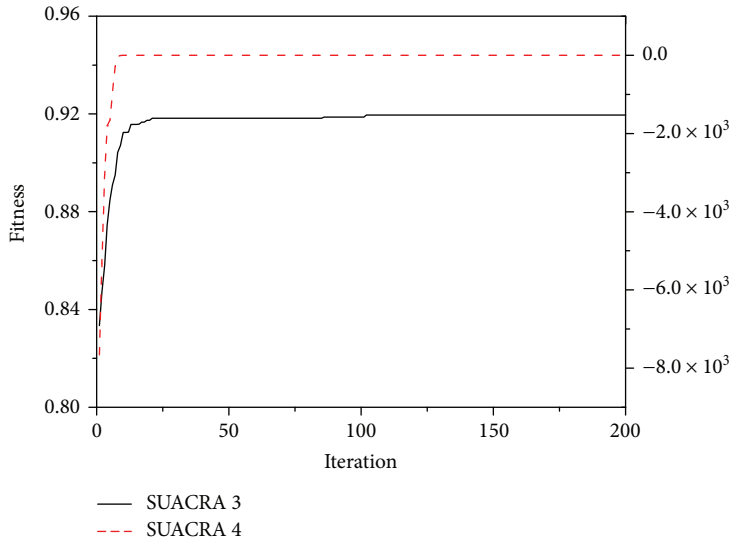


Figure 10: The fitness values throughout the optimization process of SUACRA 3 and 4.

Figure 10, the fitness values of the two SUACRAs reach the convergence points within 150 iterations.

## 5. Conclusion

In this paper, the synthesis of the sparse uniform-amplitude transmitting array is discussed. As a result, uniform exciting strategy, reduced element number, and a higher *BCE* are achieved simultaneously for the optimal MPT. Accordingly, the fabrication, maintenance and feed network design of the transmitting array are greatly simplified without loss of *BCE*. The numerical results show that the SUACRAs optimized by the proposed method have fewer elements than the random array and the stepped one on the same $BCE^{U}$. Compared to the RLUAA, the SUACRA saves 32% elements with a 1.1% higher $BCE^{U}$, while the sparsification ratio $\xi$ is improved by 12% with 0.98% decrease of $BCE^{U}$. Compared to the SAA, the SUACRA can save 29.1% with a bit higher $BCE^{U}$, and the sparsification ratio $\xi$ is improved by 9.8% with 1% decrease of $BCE^{U}$. The proposed SUACRAs have higher *BCE*s, simple array arrangement and feed network, and could be used as the transmitting array for a large-scale MPT system.

## Data Availability

The data used to support the findings of this study are available from the corresponding author upon request.

## Conflicts of Interest

The authors declare that they have no conflicts of interest.

## Acknowledgments

This work was supported by Natural Science Foundation of China (Grant no. 61271062 and Grant no. 61771300).

## References

[1] J. O. McSpadden and J. C. Mankins, "Space solar power programs and microwave wireless power transmission technology," *IEEE Microwave Magazine*, vol. 3, no. 4, pp. 46–57, 2002.

[2] X. X. Yang, "Antennas in microwave wireless power transmission," *Handbook of Antenna Technologies*, pp. 1–37, 2014.

[3] R. M. Dickinson and W. C. Brown, "Radiated microwave power transmission system efficiency measurements," Tech. Rep. 142986, Jet Propulsion Lab, California Institution of Technology, Pasadena, CA, USA, 1975.

[4] R. M. Dickinson, "Performance of a high-power, 2.388-GHz receiving array in wireless power transmission over 1.54 km," in *1976 IEEE-MTT-S International Microwave Symposium*, pp. 139–141, Cherry Hill, NJ, USA, June 1976.

[5] S. Takeshita, "Power transfer efficiency between focused circular antennas with Gaussian illumination in Fresnel region," *IEEE Transactions on Antennas and Propagation*, vol. 16, no. 3, pp. 305–309, 1968.

[6] G. Oliveri, L. Poli, and A. Massa, "Maximum efficiency beam synthesis of radiating planar arrays for wireless power transmission," *IEEE Transactions on Antennas and Propagation*, vol. 61, no. 5, pp. 2490–2499, 2013.

[7] A. K. M. Baki, N. Shinohara, H. Matsumoto, K. Hashimoto, and T. Mitani, "Study of isosceles trapezoidal edge tapered phased array antenna for solar power station/satellite," *IEICE Transactions on Communications*, vol. E90-B, no. 4, pp. 968–977, 2007.

[8] X. Li, B. Duan, L. Song, Y. Zhang, and W. Xu, "Study of stepped amplitude distribution taper for microwave power transmission for SSPS," *IEEE Transactions on Antennas and Propagation*, vol. 65, no. 10, pp. 5396–5405, 2017.

[9] A. Massa, G. Oliveri, F. Viani, and P. Rocca, "Array designs for long-distance wireless power transmission: state-of-the-art and innovative solutions," *Proceedings of the IEEE*, vol. 101, no. 6, pp. 1464–1481, 2013.

[10] X. Li, B. Duan, J. Zhou, L. Song, and Y. Zhang, "Planar array synthesis for optimal microwave power transmission with

multiple constraints," *IEEE Antennas and Wireless Propagation Letters*, vol. 16, pp. 70–73, 2017.

[11] Z. K. Chen, F. G. Yan, X. L. Qiao, and Y. N. Zhao, "Sparse antenna array design for MIMO radar using multiobjective differential evolution," *International Journal of Antennas and Propagation*, vol. 2016, Article ID 1747843, 12 pages, 2016.

[12] D. Pinchera, M. D. Migliore, F. Schettino, M. Lucido, and G. Panariello, "An effective compressed-sensing inspired deterministic algorithm for sparse array synthesis," *IEEE Transactions on Antennas and Propagation*, vol. 66, no. 1, pp. 149–159, 2018.

[13] X. Zhao, Y. Zhang, and Q. Yang, "Synthesis of sparse concentric ring arrays based on Bessel function," *IET Microwaves, Antennas & Propagation*, vol. 11, no. 11, pp. 1651–1660, 2017.

[14] P. Rocca, G. Oliveri, and A. Massa, "Innovative array designs for wireless power transmission," in *2011 IEEE MTT-S International Microwave Workshop Series on Innovative Wireless Power Transmission: Technologies, Systems, and Applications*, pp. 279–282, Uji, Kyoto, Japan, May 2011.

[15] A. F. Morabito, A. R. Laganà, and T. Isernia, "Optimizing power transmission in given target areas in the presence of protection requirements," *IEEE Antennas and Wireless Propagation Letters*, vol. 14, pp. 44–47, 2015.

[16] A. F. Morabito, "Synthesis of maximum-efficiency beam arrays via convex programming and compressive sensing," *IEEE Antennas and Wireless Propagation Letters*, vol. 16, pp. 2404–2407, 2017.

[17] Q. Guo, C. Chen, and Y. Jiang, "An effective approach for the synthesis of uniform amplitude concentric ring arrays," *IEEE Antennas and Wireless Propagation Letters*, vol. 16, pp. 2558–2561, 2017.

[18] J. Kennedy and R. Eberhart, "Particle swarm optimization," in *Proceedings of ICNN'95 - International Conference on Neural Networks*, pp. 1942–1948, Perth, WA, Australia, November-December 1995.

[19] S.-I. Kang, K.-T. Kim, S.-J. Lee, J.-P. Kim, K. Choi, and H.-C. Kim, "A study on a gain-enhanced antenna for energy harvesting using adaptive particle swarm optimization," *Journal of Electrical Engineering and Technology*, vol. 10, no. 4, pp. 1780–1785, 2015.

[20] C. Han and L. Wang, "Array pattern synthesis using particle swarm optimization with dynamic inertia weight," *International Journal of Antennas and Propagation*, vol. 2016, Article ID 1829458, 7 pages, 2016.

[21] C. A. Balanis, *Antenna Theory: Analysis and Design, Chapter 6*, John Wiley & Sons, third edition, 2005.